A five-day back trajectory climatology for Rukomechi research station (northern Zimbabwe) and the impact of large-scale atmospheric flows on concentrations of airborne coarse and fine particulate mass

Daniel Nyanganyura[a,b]*, Amos Makarau[a,c], Manny Mathuthu[a] and Franz X. Meixner[a,b]

The climatology of slow and fast air mass transport towards Rukomechi research station in northern Zimbabwe (16.1°S, 29.4°E) is examined through an analysis of 5-day kinematic back trajectories arriving at 1180 m above ground level (~850 hPa) for the period 1994–99. The trajectories are computed daily by the HYSPLIT 4 model using the National Oceanic and Atmospheric Administration's re-analysed wind fields as input. Objective classification of trajectories into different flow regimes is done using a non-hierarchical cluster algorithm that is applied to all the trajectories at once, to examine the temporal and spatial characteristics. The synoptic-scale atmospheric circulation associated with each cluster was also studied. Four major transport corridors and seven large-scale flows were found to provide an indication of source regions of the air masses and transport pathways influencing Rukomechi. The dominant transport features include (1) the late dry season to wet season eastern air flows that contribute 35% of the total flow and which are driven by an anticyclone that wraps around the subcontinent and stretches into the Mozambique Channel, (2) the late wet season to dry season southeastern pathway that accounts for 44% of the total flow and is associated with the South Atlantic anticyclone and the tropical depression in the Indian Ocean, (3) the fast (11 m s^{-1}) dry season southern flow (contributes 8%) that is driven by a continental anticyclone over South Africa coupled to a South Atlantic anticyclone, and (4) the north-northwesterly flow that contributes 6% to the total flow and is associated with the Intertropical Convergence Zone. A further, very slow (1.8 m s^{-1}) flow regime, consisting of regionally re-circulated air results from regional differential heating at the surface. Concentrations of particulate mass, measured during 1994–2000 at the Rukomechi site, are shown to be significantly correlated with the occurrence of those seven large-scale flows, which have been identified by objective trajectory classification. High particulate mass concentrations are associated only with air masses carried along the fast easterly flow, the slow southeasterly flow and the southerly flow (dry season flows); low particulate mass concentrations are exclusively found with wet season flows.

Introduction

The spreading of gaseous and particulate pollution from their sources, and its effect on the environment and climate,[1] has become an increasingly important research area in recent decades, due to interest from both scientists and the public. A comprehensive understanding of the air mass climatology of a particular geographical region is a prerequisite for evaluating transport processes and pathways of airborne material. The characterization of the different air masses arriving at a given location is a useful tool for evaluating the integrated effect of transport and meteorology on chemical climates.[2] Application of a trajectory model is the standard approach to assessing the potential contributions of distant air pollutant sources to a particular region.

In meteorological terms, a trajectory is the time-integration of the change in position of an air parcel as it is transported by the wind.[3] Air mass trajectories are typically calculated in a backward mode (path of air movement arriving at a receptor location) or forward mode (path of air movement leaving from a source location). Daily back trajectories, calculated for several years and classified according to speed and direction, usually form the air mass flow climatology of a receptor site. Development of such a flow climatology (a) improves the understanding of typical air flow patterns, (b) facilitates the comparison of the distribution of trajectories across different directions and times of the year, and (c) allows the classification of air masses in terms of the origin of sampled air. The combination of the air-flow climatology with results of chemical analysis of the sampled air is a standard tool to understand the observed temporal variations of the chemical measurements at a receptor site.

Backward trajectories have been used to explore predominant source regions of ozone, particulate matter, and regional haze for various receptor locations and time periods[4] and to establish typical flow patterns and transportation ranges.[5,6] In Africa, air mass trajectories have been used to characterize the transport of airborne particulates over equatorial eastern Africa,[7] to study the inter-regional transport of air masses in the southern hemisphere,[8] and to investigate the dominant vertical and horizontal circulation patterns over southern Africa.[9]

When calculating individual trajectories, most computational methods use (1) observed or model-derived wind data to compute horizontal components, and (2) either isobaric, kinematic or isentropic methods to determine the vertical components of the trajectory. The isobaric and isentropic approaches assume that the trajectory remains on surfaces of constant pressure and constant potential temperature, respectively, whereas the kinematic approach assumes that the trajectory moves with the vertical wind fields generated by a diagnostic or prognostic meteorological model.[10] Kinematic and isentropic methods have been compared[11,12] and the kinematic approach has been found to be preferable for trajectory modelling over southern Africa.[6,9] The kinematic trajectory approach was therefore used in the present study.

[a]Physics Department, University of Zimbabwe, P.O. Box MP167, Mt Pleasant, Harare, Zimbabwe.
[b]Biogeochemistry Department, Max Planck Institute for Chemistry, P.O. Box 3060, D-55020, Mainz, Germany.
[c]Meteorological Services Department, P.O. Box BE150, Belvedere, Harare, Zimbabwe.
*Author for correspondence: Biogeochemistry Department, Max Planck Institute for Chemistry, P.O. Box 3060, D-55020, Mainz, Germany.
E-mail: nganyura@mpch-mainz.mpg.de

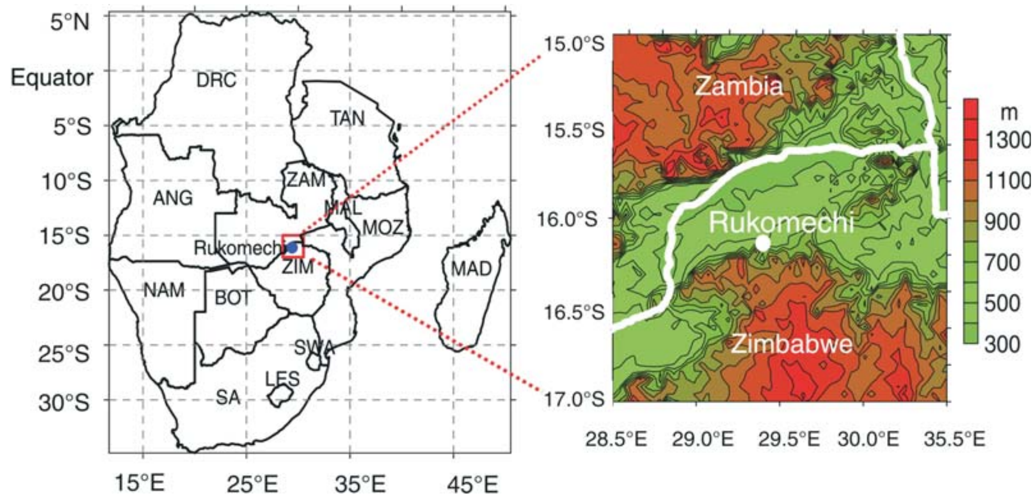

Fig. 1. The location of Rukomechi research station in Mana Pools National Park (Zambezi valley) in relation to countries of southern Africa: Democratic Republic of Congo (DRC), Tanzania (TAN), Zambia (ZAM), Angola (ANG), Malawi (MAL), Mozambique (MOZ), Zimbabwe (ZIM), Namibia (NAM), Botswana (BOT), Madagascar (MAD), Swaziland SWA), Lesotho (LES), and South Africa (SA). The right-hand figure shows the topography around Rukomechi. Contous are in metres above sea level. The white line indicates national borders. Adapted from ref. 33.

A large population of trajectories has to be classified by a cluster analysis technique to develop an air-flow climatology. Cluster analysis consists of a variety of multivariate statistical analysis methods designed to explore structures within a given data set.[13] A large set of trajectories is usually collected into groups (clusters) of similar trajectories. The main goal of trajectory cluster analysis is minimizing differences between trajectories within a cluster, and maximizing differences between clusters.[14] There are many different clustering algorithms, with great variation in the computational requirement. The most common clustering algorithm (also used in this study) is a non-hierarchical algorithm, designed for large databases requiring relatively small computational and storage requirements.[15]

The study reported here presents a 5-day back trajectory climatology for the period January 1994 to December 1999 at Rukomechi research station in northern Zimbabwe, where a meteorological station has been operating since the 1960s. Until now, similar trajectory studies in Africa have been performed only for Kenya[7,16] and southern Africa,[6] but over much shorter time periods (1991 to 1993 and only for October 1996, respectively). Furthermore, because Rukomechi is located between Kenya and South Africa, this study augments general knowledge about seasonal flows over Africa south of the equator.

Location and methods

Research site

Rukomechi research station is located in the Zambezi valley (16.1°S, 29.4°E) at a height of 510 m above mean sea level (Fig. 1), in the Mana Pools National Park (a UNESCO World Heritage site; http://whc1.unesco.org) in rural northern Zimbabwe. This location is under the influence of various air masses throughout the year, but it also experiences channelling of low-level air masses, due to the Zambezi valley. Occasionally, there are northern winds associated with the Intertropical Convergence Zone (ITCZ).[17] The ITCZ is a belt of low pressure, girdling the Earth at the equator, and is formed by the vertical ascent of warm, moist air from the adjacent latitudes above and below the equator.[18] The air is drawn into the ITCZ by the action of the Hadley cell[19] and is transported aloft by the convective activity of thunderstorms. The low pressure associated with the ITCZ is most intense over the tropical continents and the western Pacific archipelago, the main sites of ascending warm, moist air.[20] In southern Africa, the ITCZ occasionally comes close to Rukomechi and/or passes across it twice a year. This makes the research station there an important site for study of the effects of these flow changes.

Trajectory calculation

The HYSPLIT_4 (HYbrid Single Particle Lagrangian Integrated Trajectory) model[21] was used to compute backwards air mass trajectories employing the kinematic approach using the re-analysed National Oceanic and Atmospheric Administration (NOAA) data set at a resolution of 2.5° × 2.5° (latitude, longitude) as input. The HYSPLIT model is a hybrid simulation of the transport and dispersion of atmospheric pollutants over meso-scale/regional distances, performing calculation procedures that employ the Lagrangian (transport) and Eulerian (dispersion) approaches.[22,23] The Lagrangian approach describes atmospheric motion in terms of individual air parcels, moving with the air, resulting from changing synoptic circulation patterns, whereas the Eulerian method solves the advection-diffusion equation at a fixed grid point.[23,24] Five-day back trajectories were calculated on a daily basis (starting at 12:00 local time [GMT + 2 h] from January 1994 to December 1999) to sample a variety of flow regimes. Five-day back trajectories were selected because they extend far enough back in time and distance to cover the main source regions suspected of affecting northern Zimbabwe.

A starting height of 1180 m above ground level (~ 800 hPa pressure level) was chosen, because it is above the escarpment (to minimize valley channelling effects). This height was found to be within the mean annual mixed-layer depth over Rukomechi (1570 m above ground level, as determined by HYSPLIT), and also below the region's maximum of the mixed layer (*c.* 4 km[25,26]). The model computes backward trajectories for air masses arriving at Rukomechi research station with position (latitude, longitude), height above ground level, relative humidity and mixed-layer depth at every hour.

Trajectory cluster analysis

To limit the computation time, the extremely large data set of trajectories was reduced by selection of latitude and longitude information every three hours (instead of 1 h). Using a cluster algorithm, minimization of the differences among air mass trajectories in a cluster, and maximization of the differences between clusters, was achieved by minimizing the Euclidean distances between the corresponding coordinates of the individual trajectories (considering the full length of each 5-day backward trajectory). The method of Dorling *et al.*[15] was applied to determine the optimum number of clusters to retain during the cluster analysis. The root mean squared deviation (RMSD) of each trajectory from its cluster mean was calculated, starting with a large number of potential clusters (e.g. $n = 20$). Summing the RMSDs of all clusters gives the total root mean squared deviation (tRMSD) of the chosen number of potential clusters. The number of potential clusters was then reduced stepwise (by one unit) and the corresponding tRMSDs were re-calculated. A steep increase in the tRMSD was observed when a significant number of different trajectories, formerly located in distinct clusters, were put together into one cluster. Thus, the optimum number of clusters to be used for the data set was taken to be that number before the steep increase in the tRMSD.

Trajectories assigned to these clusters (groups) were taken to represent the main air-flow transport regimes over Rukomechi. Finally, the air-flow climatology for Rukomechi (in terms of direction, speed and preferential flow height) was represented by the clusters of all the 5-day back trajectories for the period January 1994 to December 1999.

Representative surface pressure maps

Both the South Atlantic and the South Indian Ocean anticyclones are subtropical high pressure cells which are linked to southern Africa. They are the semi-permanent manifestations of the subtropical part of the global circulation.[18] Together with other large-scale features, namely the ITCZ and the Congo Air Boundary[27] (the most important convergence zones north of 20°S), these anticyclones influence the climate and weather over northern Zimbabwe decisively. Consequently, the mean flow over Rukomechi results from anticyclonic surface pressure patterns, leading to predominant southeasterly winds[18,19,28] (the South-East Trades[27]). Perturbations of the mean anticyclonic circulation constitute themselves in easterly/westerly waves and lows (equatorward/poleward side of the high pressure cells), as well as in other synoptic perturbations[19,20] (that is, ridging anticyclones, tropical and extra-tropical cloud bands). Upper tropospheric flows over the subcontinent, manifested by standing (wavenumbers 3–4) and travelling (wavenumbers 5–6) wave patterns exert particular control over these perturbations,[19] as documented by zonal harmonic analysis of the 500 hPa southern hemispheric geopotential heights.[29]

Any attempt to attribute the identified trajectory clusters (see Clustering analysis below) to representative large-scale mean weather patterns (surface pressure patterns) of the subcontinent faces serious problems. The dominant oceanic high pressure cells will usually mask the smaller-scale perturbations[19,27,30] to such an extent that in composite pressure maps (based on those time periods that include the occurrence of all individual trajectories of a particular cluster) the strength of the oceanic anticyclones will overshadow the influence of these perturbations. We employed a filter mechanism, intended to select time periods of representative trajectories for a particular cluster. Because of this, meteorological data derived from the European Centre for Medium Range Weather Forecasting (ECMWF) were used to plot composite surface pressure maps, considering only those days when the individual trajectories (with longitudinal and latitudinal displacement) were found to be within 20% of the mean cluster trajectory (see Spatial and dynamic patterns of the flow).

Results and discussion

Optimization of number of clusters

The tRMSD of the trajectories gradually increased as the number of potential clusters was decreased. However, it was often difficult to identify the appropriate steep increase that could be used for cluster number optimization. The percentage change in the tRMSD from n to $n - 1$ clusters (ΔtRMSD) was therefore calculated to achieve better insight into the changes. In Fig. 2, ΔtRMSD is shown as a function of the step change of the potential cluster numbers. Reducing the number of potential clusters stepwise from 20 downwards, the first major steep increase was observed when reducing the cluster numbers from seven to six. According to Dorling *et al.*,[15] seven was identified as the optimum number of clusters for best representation of the various air flows to Rukomechi.

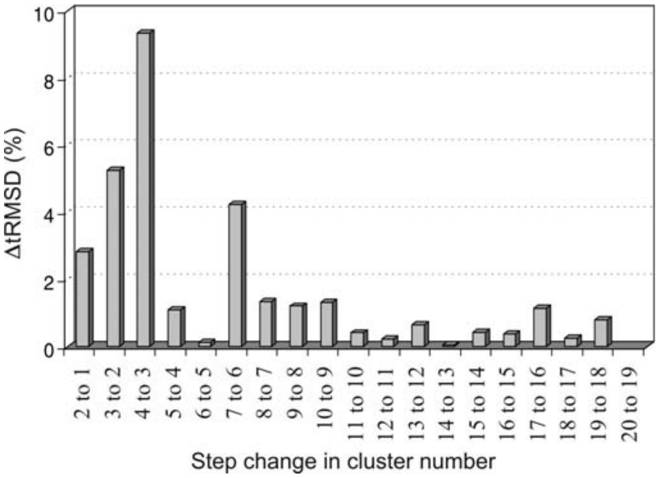

Fig. 2. Percentage change of the total root mean square deviation (ΔtRMSD) for incremental reduction (step change of one unit) of the potential cluster numbers, n (starting with $n = 20$).

Clustering analysis

Figures 3(a)–(g) illustrate how all the daily trajectories for the period of study were assigned to the seven clusters identified by the clustering algorithm. These plots give a qualitative impression of the variability of the trajectories within each cluster. Although considerable variability within each individual cluster is evident, there is ample evidence that the clustering procedure grouped the trajectories into seven clearly distinct clusters.

A median trajectory was computed for each cluster. The seven median trajectories are shown in Fig. 4, and represent the seven general air mass pathways to Rukomechi in terms of direction of flow, wind speed and the preferential transport height. The length of each median trajectory is five days and the distance between two successive data points represents a three-hour interval.

The main transport regimes to Rukomechi were (1) the eastern corridor with two easterly flows, one that originated from eastern Africa (cluster A) and another, relatively faster flow arising from northern Madagascar (cluster B); (2) the southeastern corridor also with two flows, one originating from the Indian Ocean off southern Madagascar (cluster C) and the slow flow that came from the Mozambique Channel (cluster D); (3) the southern corridor that carried air from the Atlantic Ocean round the tip of southern Africa (cluster E); (4) the north-northwest corridor (cluster F), which originated from Zambia and Angola; and (5) the local recirculation air (cluster G). The total ensemble of the trajectories for these flows is shown in Fig. 3 and the median trajectories in Fig. 4. The mean flow pathways (clusters) can easily be distinguished in terms of spatial, dynamic and temporal patterns.

Spatial and dynamic patterns of the flow

Eastern corridor. The slow easterly flow (cluster A, Fig. 4) contained all trajectories coming generally from easterly and north-

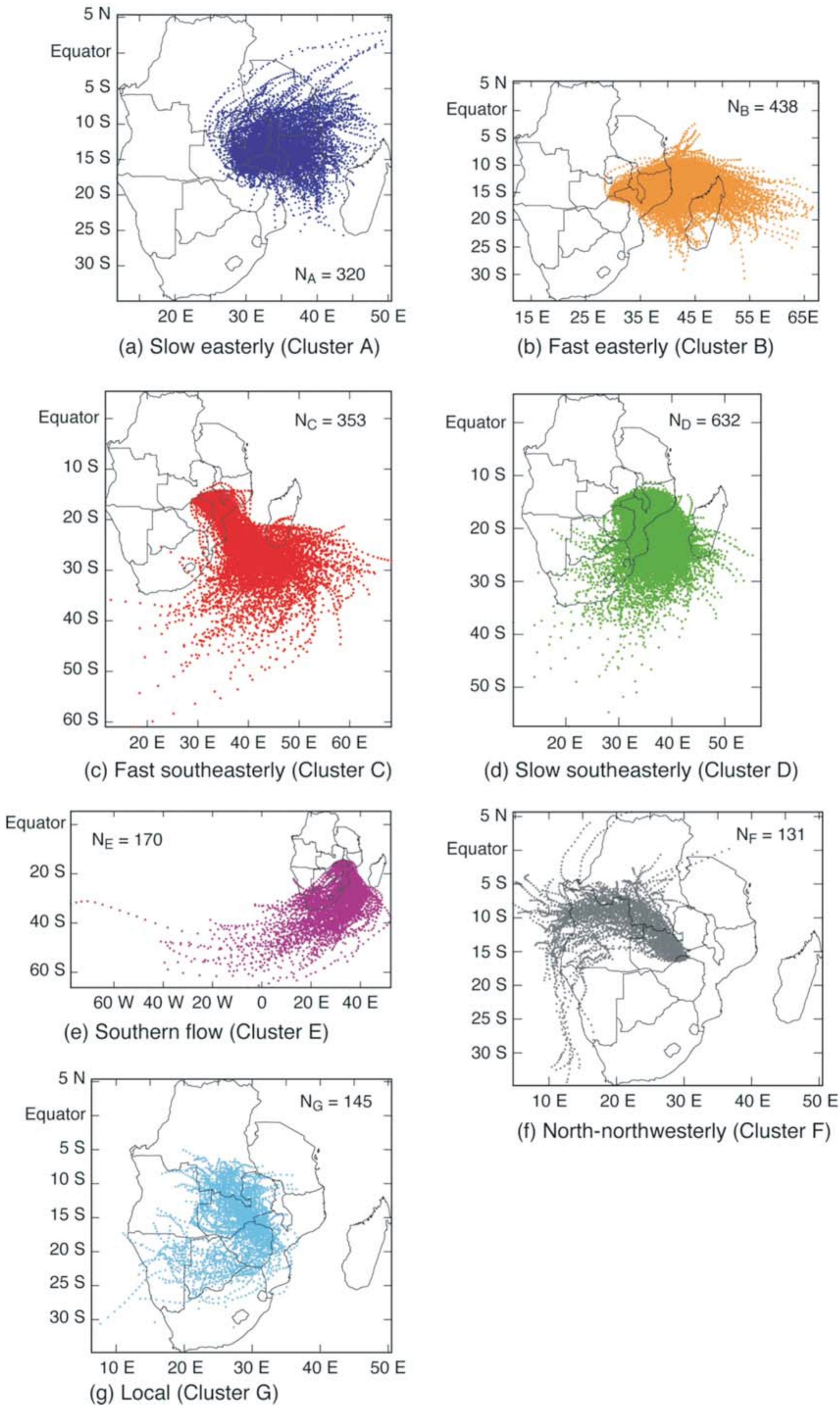

Fig. 3. Cluster membership plots of 5-day back trajectories arriving at Rukomechi station at 1180 m above ground level (~800 hPa). The data basis are trajectories (starting at 12:00 local time) for the period from January 1994 to December 1999. The seven clusters were identified by trajectory cluster analysis.

northeasterly directions, with relatively low average wind speeds of about 2.9 m s^{-1}. The fast easterly flow (cluster B, Fig. 4) brought in air from the northern part of Madagascar and northern Mozambique, with a mean wind speed of 5.4 m s^{-1}. As mentioned above, the time interval between two successive points represents a three-hour interval. It is noteworthy that the air masses in the fast easterly flow were faster over land (more spaced) than over the ocean (less spaced), contradicting the usual sea/land contrast effect, where movement of air masses was slower over land (due to surface friction) than over the sea (as in the southern corridor, cluster E). This contrast is explainable in terms of the pressure gradient force (due to the incursion of the South Indian Ocean anti-cyclone into the Mozambique Channel (see below) that overrides frictional forces.

Southeastern corridor. The air flow in this corridor also consisted of a fast (6.1 m s^{-1}, cluster C) and a relatively slow (4.1 m s^{-1}, cluster D) mean wind speed component. Air masses constituting the slow southeasterlies (cluster D) originated mainly from the Mozambique Channel, and those in the fast southeasterly corridor (cluster C) arose from the Indian Ocean off the southern coast of Madagascar.

Southern corridor. Air flow to Rukomechi from the South Atlantic round the tip of southern Africa is shown by the mean trajectory of cluster E (Fig. 4). Bearing in mind that the length of each trajectory is five days, the existence of (very) long trajectories in the southern corridor shows that the fastest flow of air masses to Rukomechi occurred along this pathway (average wind speed of 10.6 m s^{-1}). Over the ocean, average speed was 12.1 m s^{-1}, which declined to about 7.1 m s^{-1} as soon as the air entered the continent (enhanced surface friction) and is channelled through the Zambezi valley. Air parcels in this flow will have turned through an angle of about 180° by the time that they reached the research station.

Furthermore, mean trajectories in the southern (and southeastern) corridors all showed anticyclonic curvature when arriving from the east at Rukomechi, suggesting that the airflow associated with these pathways is part of the anticyclonic recirculation modes of air over southern Africa.[9]

North-northwestern corridor. Predominantly continental air from Zambia and Angola reached the receptor site in this corridor; the corresponding mean trajectory (average speed of 4.1 m s^{-1}) is shown in Fig. 4 as cluster F. Some of the individual trajectories in this corridor (Fig. 3) reached Rukomechi from the Atlantic Ocean, and the general trajectories' curvature tended to be cyclonic, in contrast to those in the eastern, southeastern, and southern corridors, where anticyclonic flows prevailed.

Local winds. Air flows that have been assigned to cluster G generally looped around Rukomechi with a least mean wind speed of 1.8 m s^{-1}. Like cluster F, the transport regime of cluster G brought mainly continental air to Rukomechi.

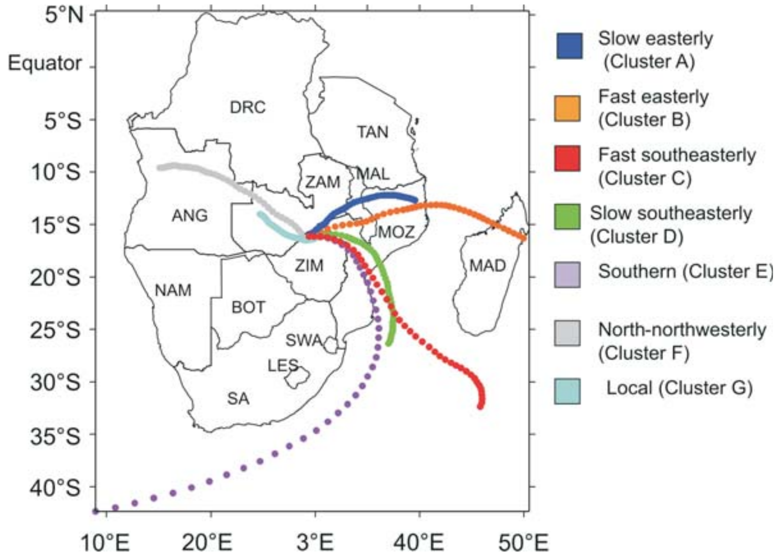

Fig. 4. Mean trajectories for clusters A–G (see Fig. 3) arriving at Rukomechi station at 1180 m above ground level (~800 hPa) for the period from January 1994 to December 1999. The southern African countries are as explained in Fig. 1.

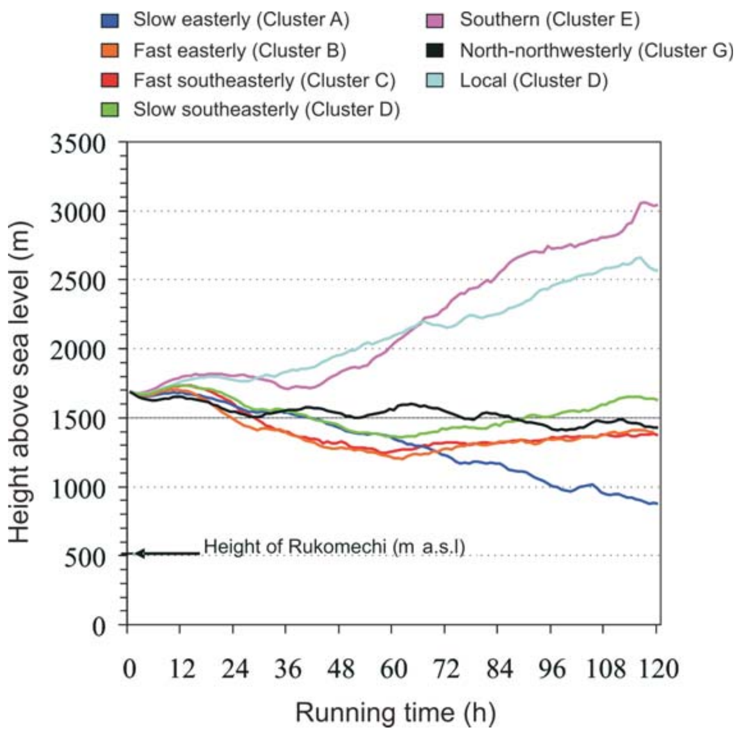

Fig. 5. Median height (above sea level) of all trajectories in an individual cluster (A to G) as a function of trajectory running time (5 days).

Figure 4 shows the horizontal pathways of the clusters' median trajectories, whereas Fig. 5 depicts the median height (metres above ground level) of the median trajectories during the five days before their arrival at the receptor site.

The fast easterly (cluster B), the fast (cluster C) and slow (cluster D) southeasterly, and the north-northwesterly (cluster F) flows showed a tendency of persistent horizontal transport at an average height of about 850 m above ground level. As was to be expected, the fast southern winds (cluster E) subsided from higher altitudes; this was associated with the descent of air along isentropic surfaces sloped down towards the equator.[31] Similar behaviour, but less pronounced, was observed for the local trajectories associated with cluster G. The slow easterly (cluster A) is characterized by rising air masses.

The air-flow corridors' contributions to the total air flow to Rukomechi are shown in Fig. 6. The eastern corridor (clusters A and B) contributed 35%, whereas the southeastern corridor (clusters C and D) accounted for 44% to the total flow. The dominance of clusters C and D indicates the strong influence of the south-east trade winds that generally dominate the air flow between 30°S and the equator.[28] The high speed southern flow (cluster E) contributed to 8% of the cases and the north-northwest flow (cluster F, associated with the ITCZ) provided 6% to the total air flow to Rukomechi over the six years.

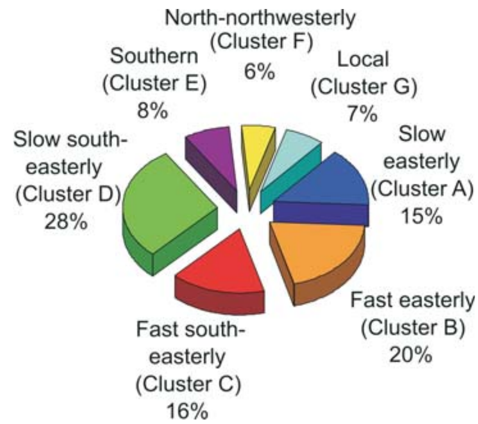

Fig. 6. Percentage contribution of the seven identified trajectory clusters (A–G) to the total air flow to Rukomechi research station for January 1994 to December 1999.

Temporal distribution of trajectories

Temporal distributions of air flow were investigated in terms of mean annual cycles with particular consideration of subtropical seasons. Using 60% relative humidity as baseline, dry and wet seasons at Rukomechi were defined as periods from mid-April to mid-November and from mid-November to mid-April, respectively (Fig. 7). The end of the wet season/beginning of the dry season (mid-April) was defined as the period when the median relative humidity curve crossed the 60% line for the first time, whereas the end of the dry season/beginning of the wet season was defined as the time when a sudden increase in relative humidity was noted (mid-November). Median relative humidity was derived from hourly measurements of relative humidity at Rukomechi between 1992 and 2000. Monthly percentage contributions of each cluster to the total air flow (January 1994 to December 1999) were calculated and are presented in Fig. 8.

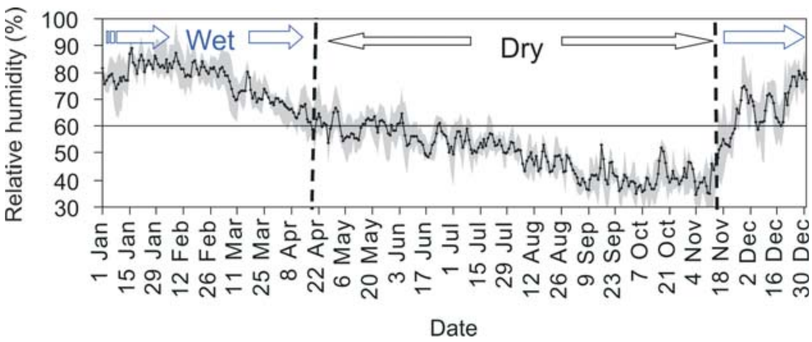

Fig. 7. Median (line) and inter-quartile range (shaded grey) of relative humidity derived from hourly measurements at Rukomechi from January 1992 to December 1999. The end of the wet season/beginning of the dry season was defined as the time when the median relative humidity curve crossed the 60% line for the first time whereas the end of the dry season/beginning of the wet season was defined as the period when a sudden increase in relative humidity was noted.

The slow southeasterly flow (cluster D) alone contributed most (28%, see Fig. 6) to the total flow, and was prevalent all year round, indicating again the general influence of the south-east trade winds. This flow was more evident from the onset of the dry season (April) to September, when its monthly contribution was always above 3%; during the rainy season, particularly in January and February, the monthly contribution dropped to 1.3% and 0.98%, respectively.

The fast easterly flow (cluster B), the second-largest individual contribution to the total flow (20%, see Fig. 6), started to appear significantly in August (middle of the dry season). It reached its maximum monthly contribution in November (4.7%), and underwent rapid decay to 2.2% in the early wet season (December). Although there was a sudden fall of the fast easterlies in December, the flow to Rukomechi was still predominantly easterly, particularly due to the contribution of slow easterly flow (cluster A).

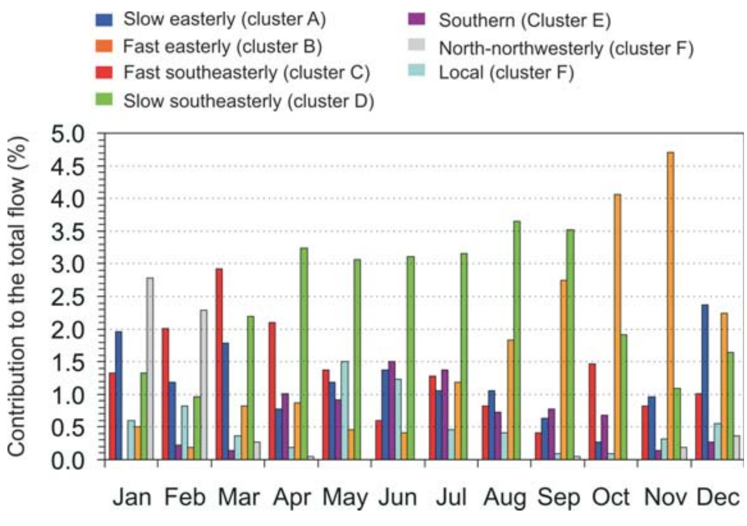

Fig. 8. Percentages of the monthly long-term occurrences of trajectories in each cluster for the air masses arriving at Rukomechi for the period January 1994 to December 1999.

The north-northwesterly flow (cluster F) appeared significantly only in the mid-wet season (January and February), when its monthly percentage contributions were 2.8% and 2.3%, respectively.

The fast southeasterly flow (cluster C), third-largest contributor to the total flow (16%, see Fig. 6), became most active from the mid-wet season onwards and contributed most to the air mass transport at the end of the rainy season (2.9% in March, see Fig. 8). Strengthening of this flow at the expense of the north-northwestely (cluster F) is indication that the fast southeasterlies played a major role in the final northwards movement of the ITCZ (see next section). As the fast southeasterlies (cluster C) weakened at the change between wet and dry seasons, the slow southeasterlies (cluster D) then became the main contributor to the total flow, and an annual cycle of southeastern, eastern, and the north-northwestern then recommenced. Moreover, it is interesting to note that for paired air corridors (eastern and southeastern), the dominance of fast transports was always followed immediately by slow transports. This phenomenon may be due to the dynamics of synoptic weather systems that were responsible for the different flow patterns.

The fastest air transport (cluster E), originating from the South Atlantic (Fig. 4), was limited to the southern hemisphere's winter season (June to August). The highest monthly contribution was 1.5% (June), whereas least contributions occurred in the middle of the rainy season, particularly in December and January.[32,33] Although trajectories of cluster E contributed only 8% to the total flow, they may comprise a significantly influential pathway of air pollutant transport to Rukomechi, because they were the longest and fastest. They frequently passed over most of the industrialized regions of South Africa (see Fig. 3), and they occurred during the cold and relatively dry season.

Local winds (cluster G), contributing 7% to the total flow (see Fig. 6), originated mainly from the north-northwest to south-southwest and the fetch of this flow describes a semi-circle of 600 km radius. Local winds significantly influenced the flow during the beginning of the dry season, when its monthly contribution was highest in May (1.5%).

Air mass flows and surface pressure systems over southern Africa

The occurrence of selected individual trajectories of each cluster (within 20% of the median cluster trajectory, see Representative surface maps and Spatial dynamic patterns of the flow, above) governed the construction of composite surface-pressure maps. These are shown, together with median cluster trajectories, in Fig. 9a–f. The large-scale pattern of anticyclonic and cyclonic pressure systems may appear to be different from those shown in relevant textbooks,[18,19,27] constituting climatologically mean situations for July/January, or southern hemisphere winter/summer, respectively. However, the time averaging periods of our composite surface-pressure maps comprise events of trajectory occurrence that generally did not follow strict seasonal classification (see Fig. 8).

The easterlies (clusters A and B) were influenced by a ridge of high pressure wrapping around the subcontinent, and a continental cyclone developed between the borders of Angola and Zambia (Fig. 9a and b). The incursion of the high pressure system into the Mozambique Channel pushed the flows to Rukomechi further north, and finally easterly, as they approached the study site. This incursion accelerated the air, giving it an unusual higher speed over land than over sea (see cluster C, Fig. 4). The strength and position of the pressure cells may differentiate the two easterly flows. The high pressure ridge reached the central part of the Mozambique Channel for the fast easterly flow (cluster B). This flow was also associated with a continental low pressure cell situated southeast of the Democratic Republic of Congo, and a tropical depression located in the Indian Ocean south of Madagascar (Fig. 9b). In the case of the slow easterlies (cluster A), the incursion of a high pressure system remained south of the Mozambique Channel (Fig. 9a), and a continental cyclone was found around the Caprivi Strip, stretching along the subcontinent to the southern part of South Africa (Fig. 9a).

The fast southeasterly flow (cluster C) was influenced mainly by the South Atlantic Ocean Anticyclone (SAOA), which is centred off the southern coast of South Africa, and exerted influence also in northwest South Africa and southern Zimbabwe (Fig. 9c). The other dominant feature is the Indian Ocean tropical depression centred south of Madagascar. Observing the pressure pattern's development over a number of consecutive days shows that the SAOA strengthens as it moves eastwards and curves around South Africa, while the low pressure centre moves northeastwards and locates in the Indian Ocean. The development and positioning of these cells bring fast southeasterly air towards Rukomechi (Fig. 9c).

The slow southeasterly flow (cluster D) was characterized by generally higher surface pressure levels over the region (minimum 1002 hPa) and two anticyclones, one far southwest in the Atlantic (1034 hPa) and the other southeast in the Indian Ocean (1030 hPa) (Fig. 9d). Both subtropical anticyclones were too distant to have direct influence on the flow to the receptor site. The slow southeasterly is therefore thought to be controlled by unperturbated and steady south-east trade winds,[34] as the ITCZ is also positioned far in the north during the dry season (April to September, see Fig. 8).

The southern flow (cluster E) was characterized by a continental anticyclone, which was centred over South Africa/southern Zimbabwe. The continental anticyclone was connected to the SAOA (at 5°E) by a ridge of high pressure (Fig. 9e). Time analysis of the sequence leading to this pressure pattern indicated that the continental anticyclone 'buds off'[35] from the SAOA. The coupled system of high pressure cells was responsible for the dominating winds coming from the South Atlantic. A tropical depression between the South Atlantic and South Indian Ocean anticyclones also assisted in drawing winds from the South Atlantic; but as air masses approached the coast, the main driving force was the continental anticyclone over South Africa. Apart from the effect of enhanced overland friction, the relatively weak continental anticyclone could be another explanation of why the wind speed of this flow decreased as it approached the coast en route to northern Zimbabwe.

The continental air flow (cluster F) may be driven by the continental low pressure cell sitting over western Zambia, bringing clockwise winds around to Rukomechi. Though it is a weak tropical depression, its presence may also be responsible for the cyclonic circulation of air over the entire subcontinent. The subtropical high pressure belt (along 40°S) shows marked cells of high pressure on either ocean, but this is too distant to influence the flow over Rukomechi. We conclude that the north-northwesterly flow was mainly due to the low pressure system caused by the ITCZ, which was very near to Rukomechi at this time (January/February, mid-wet season).

There were no distinct patterns of surface pressure associated with the flow patterns of the local winds (cluster G), the reason for exclusion from Fig. 9. We nevertheless suggest that air motions with this flow regime appeared be due to regional differential heating at the surface (A. Makarau, pers. comm.).

The impact of air mass transport on particulate mass concentration

The air mass climatology described above for Rukomechi between 1994 and 1999 has facilitated an evaluation of the impact of large-scale transport processes on observed particulate mass (PM) concentrations at the Rukomechi site.[32] Atmospheric particles were sampled at the station using a stacked filter unit[36] that collected two separate size fractions ['coarse' (2–10 μm diameter) and 'fine' (<2 μm diameter)] between September 1994 and January 2000. The samples were analysed for PM, carbon black, and chemical composition (47 specific elements).[33] The context of this paper constrains us to focus on only one aspect, namely, the particulate mass (coarse and fine) of this airborne material. The temporal variations of coarse and fine PM concentrations (median monthly concentrations) are given in Fig. 10. Concentrations of coarse and fine particulates show remarkable seasonal features, with a distinct annual cycle. High PM concentrations occurred during the dry period (mid-April to mid-November), whereas low concentrations were found in the

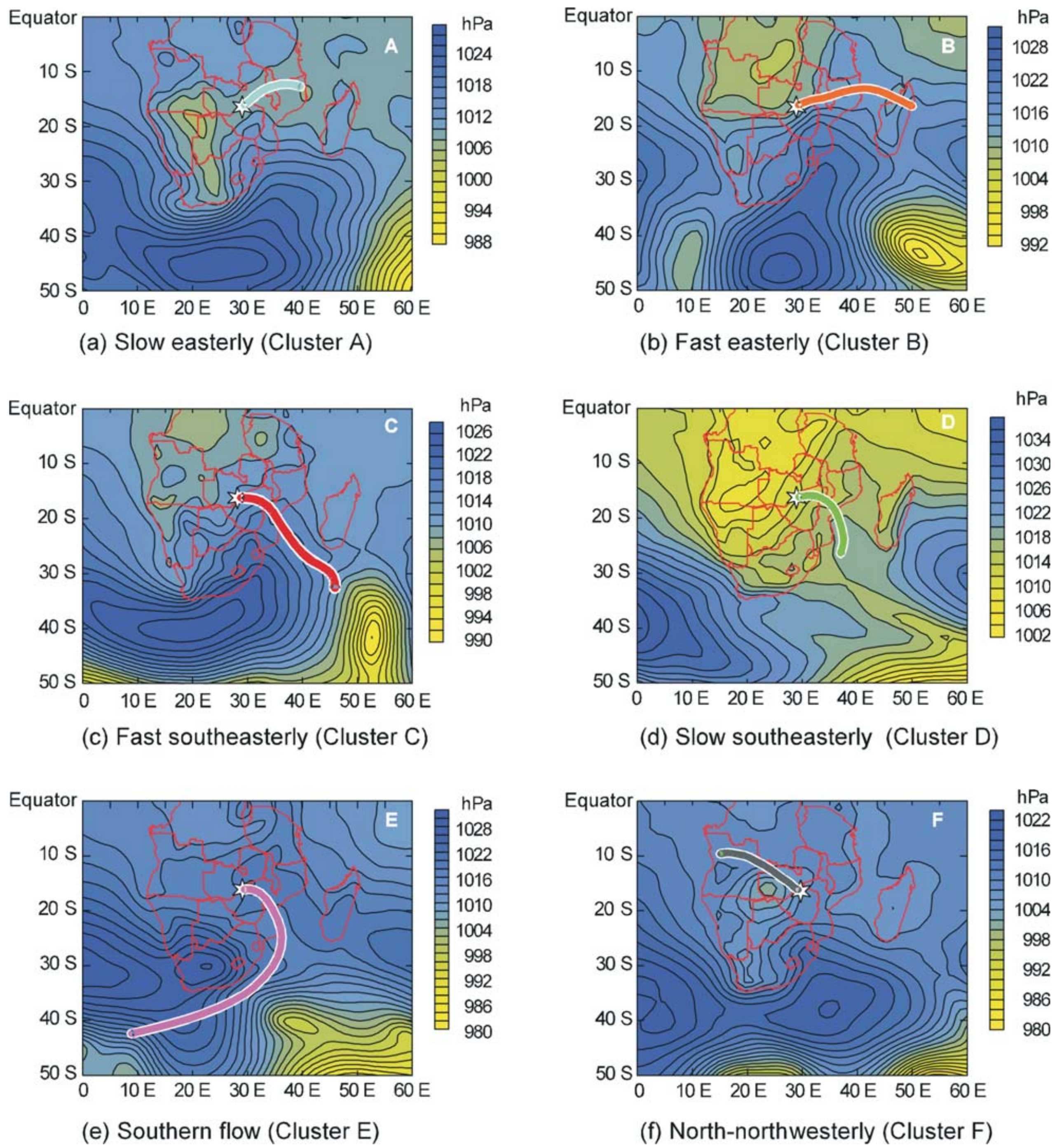

Fig. 9. Composite surface-pressure patterns that characterize the air mass flows to Rukomechi station for the period of January 1994 to December 1999.

wet season (mid-November to mid-April). While fine PM originates mainly from burning biomass, coarse PM is attibuted to airborne inorganic microparticles.[32,33] Low wet season PM concentrations are attributed to typical wet season surface and tropospheric conditions that suppress particulate emissions, as well as accelerate the removal of particulates from the atmosphere by wet deposition.[32]

At a first appearance, temporal variations of PM concentrations at Rukomechi were due only to changes in source emission patterns and climatological conditions of the season. However, the impact of directional winds can also be studied by correlating trajectory cluster occurrence and PM concentration data. The relationship between trajectory flow sectors and PM concentrations is summarized in Fig. 11. There is a clear correlation of both coarse and fine PM concentrations (expressed as long-term means) with the seven flow sectors that are identified in Spatial and dynamic patterns of the flow (see above). High PM concentrations (coarse: 9–13 μg m^{-3}; fine: 13–18 μg m^{-3}) (Fig. 11, upper panel) were associated with dry season air flows (fast easterly, slow southeasterly, southern), low PM concentrations (coarse: <7 μg m^{-3}, fine: <9 μg m^{-3}) (Fig. 11 lower panel) reached Rukomechi with the remaining four wet season air flows.

The dry season flows yielded positive correlations between monthly trajectory occurrence and mean monthly PM concentrations. For coarse PM, correlation coefficients are 0.44, 0.63 and 0.45 for the fast easterly, the slow southeasterly and the southern flows, respectively; for fine PM, the corresponding correlation coefficients are 0.63, 0.45 and 0.39, respectively. These high positive correlations indicate the strength of a linear relationship between direction of flow and PM concentrations during high-concentration episodes. The mean dry season PM concentrations were also found to be above the long-term (1994–99) average concentrations of coarse and fine PM, which were 9.2 μg m^{-3} and 11.4 μg m^{-3}, respectively. The highest monthly mean concentrations of coarse (13.4 μg m^{-3}) and fine (17.5 μg m^{-3}) PM appeared in the fast easterly flow (Fig. 11, upper panel). The fast easterly is a dry to early wet-season flow, with highest frequency occurring from August to December (Fig. 8). Source apportionment of Rukomechi airborne particulates[33] showed that biomass burning activities accounted mostly for fine PM, and the peak period of the fast easterly coincided with the biomass burning season (August–November) in the subcontinent.[32] The fast easterly flow also tended to suspend soil dust particles from the bare and dry ground during the dry season.

Also shown in Fig. 11 are the percentage PM concentrations that were above the 75th percentile of the corresponding monthly mean (coarse and fine) concentrations. For both coarse and fine PM, high percentages were found in the slow southeasterly flow (coarse 37%; fine 39%), the fast easterly flow (coarse 33%; fine 32%), and the southern flow (coarse 14%; fine 12%). The preferential transport heights (Fig. 5) of these dry season air masses were within the southern African atmospheric mixing layer,[32,34] which made them very susceptible to high particulate mass loading.

There was only a small PM loading along the wet season flows (slow easterly, fast southeasterly–northwesterly and local flows). These air masses were associated with concentrations that were less than long-term mean monthly concentrations, and their occurrences were significantly and negatively correlated with the mean monthly concentrations of both coarse and fine PM, with the exception of the local flow (–0.33 to –0.37; coarse/fine). Corresponding correlation coefficients range between –0.52 and –0.75. The relatively high percentage (10% of cases that were above the 75th percentile of monthly mean PM concentration) along the slow easterly flow may be a result of biomass burning that occurred during prolonged mid-season dry spells.[37]

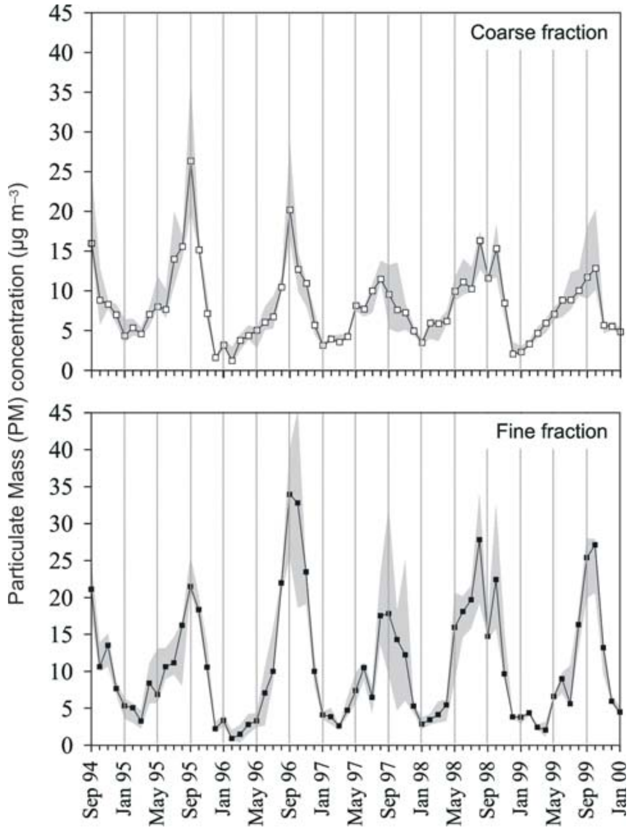

Fig. 10. Temporal variation of the long-term (1994–2000) coarse (upper panel) and fine (lower panel) PM concentrations for the Rukomechi site (grey shading indicates corresponding inter-quartile ranges).

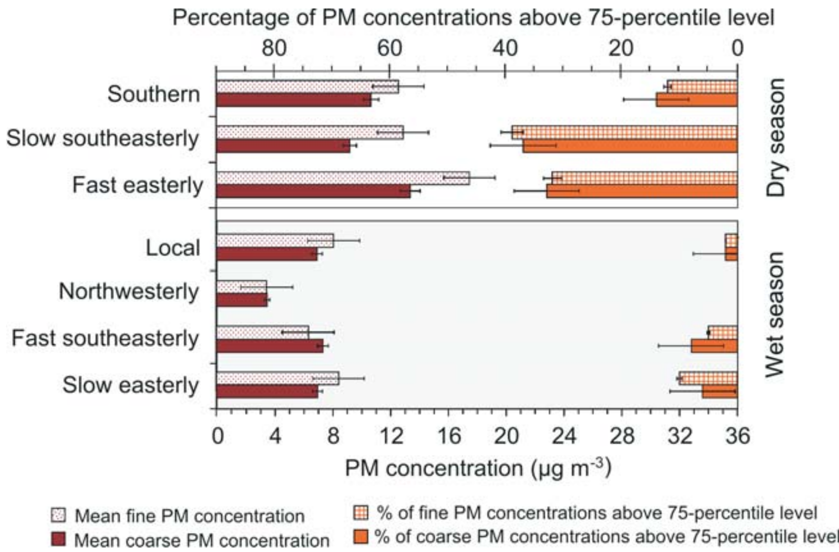

Fig. 11. Monthly mean concentrations of coarse and fine PM (lower *x*-axis; left side bars) along the seven major air flows identified for Rukomechi; the percentage of cases when PM concentrations were found to be above the 75th percentile level of the mean monthly concentration are also shown (upper *x*-axis; right side bars); error bars indicate standard deviations.

Summary and conclusions

The analysis of 5-day backward trajectories has established a six-year (January 1994 to December 1999) climatology for Rukomechi research station in northern Zimbabwe. We regard this as the first investigation of its kind at the latitude halfway between the equator and South Africa, where related studies have been reported. Classification of the trajectories by objective cluster analysis revealed pathways and origins of air parcels, as well as the pressure systems associated with each of the flows. Four corridors and seven major flows were identified, through which air masses reach Rukomechi:

(1) The eastern corridor that brings in air from northern Madagascar and Mozambique, driven by an anticyclone wrapping around the subcontinent, but sometimes stretching into the Mozambique Channel. The eastern corridor revealed both fast and slow flows. A fast flow component (5.4 m s^{-1}) was more prevalent during the end of the dry season to the beginning of the wet season (October/November), whereas a relatively slow flow component (2.9 m s^{-1}) was generally present during the mid-wet season (December/January). Both flows of the eastern corridor accounted for a 35% contribution to the total flow to Rukomechi.

(2) The southeastern corridor, through which most air flowed to Rukomechi (44%). Air masses in that corridor originated

from the Indian Ocean, south of Madagascar and also revealed a fast (6.1 m s^{-1}) and a relatively slow (4.1 m s^{-1}) wind component that contributed more dominantly in March (wet season) and April–September (dry season), respectively. The fast southeasterly flow was driven mainly by a South Atlantic anticyclone and the Indian tropical depression, while the slow component was mainly a result of the general global air circulation.

(3) The southern corridor, most active during the southern hemisphere winter (June–August), brought air from the South Atlantic around the tip of South Africa. This flow revealed the fastest air masses (10.6 m s^{-1}) and its contribution to the total flow was 8%. A continental anticyclone over South Africa, coupled to an anticyclone in the Atlantic, was the main surface feature associated with these fast winds.

(4) North-northwesterly flow from Zambia and Angola brought air during the mid-wet season, and accounted for 6% of the total flow to Rukomechi. The ITCZ, expressed as a band of relatively low pressure over the subcontinent, influenced mainly these air masses.

Lastly, the occurrence of regionally re-circulated air (7% of the total flow) was slightly enhanced in June and July, but never dominated any monthly contribution. We could not attribute any pronounced surface pressure system to this flow regime. It may well have arisen from the differential heating at the surface.

Concentrations and chemical composition of airborne particulate material were measured between September 1994 and January 2000. The particulate mass concentrations (coarse and fine size fractions) over Rukomechi clearly depended on the season and the direction of air flows. Of the seven identified flows, only the three dry season flows (fast easterly, slow southeasterly, and southerly) were associated with air masses that carried high levels of particulates (both coarse and fine). Highest PM concentrations (in excess of 10 μg m^{-3}) were transported with the fast easterly flow, while the largest numbers of air masses containing high PM concentrations occured in association with the slow southeasterly flow. The wet season flows (slow easterly, fast southeasterly, north-northwesterly, and local) carried relatively clean air masses (<9 μg m^{-3}) as southern African wet season conditions suppressed surface emissions of particulates, and accelerated their removal from the atmosphere by wet deposition.

More detailed studies have been undertaken,[32] and are still in progress, to show how the large-scale flows (identified in this work) carrying air masses originating from different part of the southern African subcontinent at different times of the year, can influence the chemical composition of airborne particulates over northern Zimbabwe. We anticipate that the potential for substantial scientific progress in this direction will include the combination of meteorological analysis (based on objective classification of long-term period trajectories arising from this work) and chemical analysis (identification and quantification of dust particles, their compositional analysis, and receptor-based source apportionment by principal component analysis[33]).

We gratefully acknowledge the financial support from the German Academic Exchange Service (DAAD) and the Max Planck Society (partially through the Max Planck International Research School) for this research. We thank W. Maenhaut (Institute of Nuclear Sciences, University of Gent, Belgium) and his group for providing the particulate mass data. We are indebted to H. Wernli (Institute of Atmospheric Sciences, University of Mainz) for his valuable help during the preparation of the manuscript, and the European Centre for Medium Range Weather Forecasting for providing data for plotting the surface pressure maps. We also thank A. Stohl for his assistance and guidance with the trajectory cluster analysis. The authors gratefully acknowledge the NOAA Air Resources Laboratory for the provision of the HYSPLIT transport and dispersion model and READY website (www.arl.noaa.gov/ready.html) used in this paper.

Received 21 April 2006. Accepted 31 January 2008.

1. Pöschl U. (2005). Atmospheric aerosols: Composition, transformation, climate and health effects. *Atmos. Chem.* **44**, 7520–7540.
2. Dorling S.R. and Davies T.D. (1995). Extending cluster-analysis – synoptic meteorology links to characterize chemical climates at 6 northwest European monitoring stations. *Atmos. Environ.* **29**(2), 145–167.
3. Doty K.G. and Perkey D.J. (1993). Sensitivity of trajectory calculations to the temporal frequency of wind data. *Mon. Wea. Rev.* **121**(2), 387–401.
4. Poirot R.L. and Wishinski P.R. (1986). Visibility, sulfate and air-mass history associated with the summertime aerosol in northern Vermont. *Atmos. Environ.* **20**(7), 1457–1469.
5. Harris J.M. (1992). An analysis of 5-day midtropospheric flow patterns for the South Pole – 1985–1989. *Tellus Ser. B – Chem. Phys. Met.* **44**(4), 409–421.
6. Tyson P.D. and D'Abreton P.C. (1998). Transport and recirculation of aerosols off southern Africa – Macroscale plume structure. *Atmos. Environ.* **32**(9), 1511–1524.
7. Gatebe C.K. *et al.* (2001) Characterization and transport of aerosols over equatorial eastern Africa. *Global Biogeochemical Cycles* **15**(3), 663–672.
8. Sturman A.P. *et al.* (1997) A preliminary study of the transport of air from Africa and Australia to New Zealand. *J. R. Soc. N. Zeal.* **27**(4), 485–498.
9. Garstang M. *et al.* (1996). Horizontal and vertical transport of air over southern Africa. *J. Geophys. Res. – Atmospheres* **101**(D19), 23721–23736.
10. Rolph G.D. *et al.* (2002). NOAA Air Resources Laboratory, ReadySite overview. Online at: www.arl.noaa.gov/readytour.html
11. D'Abreton P.C. (1996). Lagrangian kinematic and isentropic trajectory models for aerosol and trace gas transport studies in southern Africa. *S. Afr. J. Sci.* **92**, 157–160.
12. Fuelberg H.E. *et al.* (1996). TRACE a trajectory intercomparison. 2, Isentropic and kinematic methods. *J. Geophys. Res. – Atmospheres* **101**(D19), 23927–23939.
13. Romesburg C.H. (1984). *Cluster Analysis for Researches.* Lifetime Learning, Belmont.
14. Harris J.M. and Kahl J.D. (1990). A descriptive atmospheric transport climatology for the Mauna Loa Observatory, using clustered trajectories. *J. Geophys. Res. – Atmospheres* **95**(D9), 13651–13667.
15. Dorling S.R. *et al.* (1992). Cluster Analysis – a technique for estimating the synoptic meteorological controls on air and precipitation chemistry – Method and applications. *Atmos. Environ. Part A – General Topics* **26**(14), 2575–2581.
16. Gatebe C.K. *et al.* (1999). A seasonal air transport climatology for Kenya. *J. Geophys. Res. – Atmospheres* **104**(D12), 14237–14244.
17. Gedzelman S.D. (1985). Atmospheric circulation systems. In *Handbook of Applied Meteorology*, ed. D.D. Houghton. John Wiley, New York.
18. Asani G.C. (2005). *Tropical Meteorogy.* Praveen Printing Press, Pune.
19. Preston-White R.A. and Tyson P.D. (1993). *The Atmosphere and Weather of Southern Africa.* Oxford University Press, Cape Town.
20. Makarau A. (1995). Intra-seasonal oscillatory modes of the southern Africa summer circulation. Unpubl. rep., Department of Oceanography, University of Cape Town.
21. Draxler R.R. (1996). Boundary layer isentropic and kinematic trajectories during the August 1993 NARE intensive. *J. Geophys. Res. – Atmospheres* **101**, 229, 255–229, 268.
22. Draxler R.R. and Hess G.D. (1998). An overview of the HYSPLIT_4 modelling system for trajectories, dispersion and deposition. *Aust. Met. Mag.* **47**(4), 295–308.
23. Draxler R.R. and Hess G.D. (1997). *Description of the Hysplit_4 modeling system.* NOAA Tech Memo ERL. ARL.
24. Seinfeld S.H. and Pandis S.N. (1998). *Atmospheric Chemistry and Physics: From Air Pollution to Climate Change.* John Wiley, New York.
25. Anderson B.E. *et al.* (1996). Aerosols from biomass burning over the tropical South Atlantic region: Distributions and impacts. *J. Geophys. Res.–Atmospheres* **101**(D19), 24117–24137.
26. Tyson P.D. *et al.* (1996). Large-scale recirculation of air over southern Africa. *J. Appl. Met.* **35**(12), 2218–2236.
27. van Heerden J. and Hurry L. (1995). *Southern Africa's Weather Patterns.* Acacia, Pretoria.
28. Ahrens C.D. (2002). *Meteorology Today: An Introduction to Weather, Climate, and the Environment.* Brooks Cole, Pacific Grove.
29. Trenberth K.E. (1979). Interannual variability of the 500 mb zonal mean flowing the southern hemisphere. *Mon. Wea. Rev.* **107**, 1515–1524.
30. Torrance J.D. (1981). *Climate Handbook of Zimbabwe.* Zimbabwe Meteorological Services, Harare.
31. Holton J.R. (1993) *An Introduction to Dynamic Meteorology.* Academic Press, San Diego.
32. Nyanganyura D. (2006). *Atmospheric aerosol particles and transport: a climatological perspective for Zimbabwe.* Unpubl. rep., Physics Department, University of Zimbabwe.
33. Nyanganyura D. *et al.* (2007). The chemical composition of tropospheric aerosols and their contributing sources to a continental background site in northern Zimbabwe from 1994 to 2000. *Atmos. Environ.* **41**(12), 2644–2659.
34. Tyson P.D. *et al.* (1996). An air transport climatology for subtropical southern Africa. *Int. J. Climatol.* **16**(3), 265–291.
35. Hattle J. (1972). *Wayward Winds.* Longman, London.
36. Hopke P.K. *et al.* (1997). Characterization of the Gent stacked filter unit PM10 sampler. *Aerosol Sci. Technol.* **27**(6), 726–735.
37. Makarau A. (1999). Zimbabwe's climate: Past, present and future. In *Water for Agriculture in Zimbabwe: Policy and Management Options for the Smallholder Sector,* eds E.A. Manzungu *et al.* University of Zimbabwe Publications, Harare.